Electronic Supplementary Information

Impact of positive charge and ring-size on interactions of calixarenes with DNA, RNA and nucleotides

Ivona Krošl[a], Ena Otković[a], Ivana Nikšić-Franjić[a], Benoit Colasson[b], Olivia Reinaud[b], Aleksandar Višnjevac[a], and Ivo Piantanida[a*]

*

[a] Ruđer Bošković Institute, Bijenička Cesta 54, 10000 Zagreb, Croatia;
[b] Université de Paris - Laboratoire de Chimie et Biochimie, CNRS UMR 8601, 45 rue des Saints Pères, 75006 Paris, France.
*****Correspondence: pianta@irb.hr (I.P.); Tel.: +385-1-4571-326

CONTENTS:

1. Table S1: Structural features of selected nucleic acids.[1,2]

Structure type	Groove width [Å]		Groove depth [Å]	
	major	minor	major	minor
poly A- poly U (A-helix)	**3.8**	10.9	13.5	2.8
ct-DNA (B-helix)	11.7	**5.7**	8.5	7.5
$(dGdC)_n$ (B-helix)	13.5	9.5	10.0	7.2
$p(dAdT)_2$ (B-helix)	11.2	**6.3**	-	-
pdA – pdT (C-helix)	11.4	**3.3**	-	-

[1] Saenger, W. *Principles of Nucleic Acid Structure*; Springer-Verlag, New York, 1983.
[2] Cantor, C. R.; Schimmel, P. R. *Biophysical Chemistry* 1980, **3**, 1109-1181.

2. Spectrophotometric characterization:

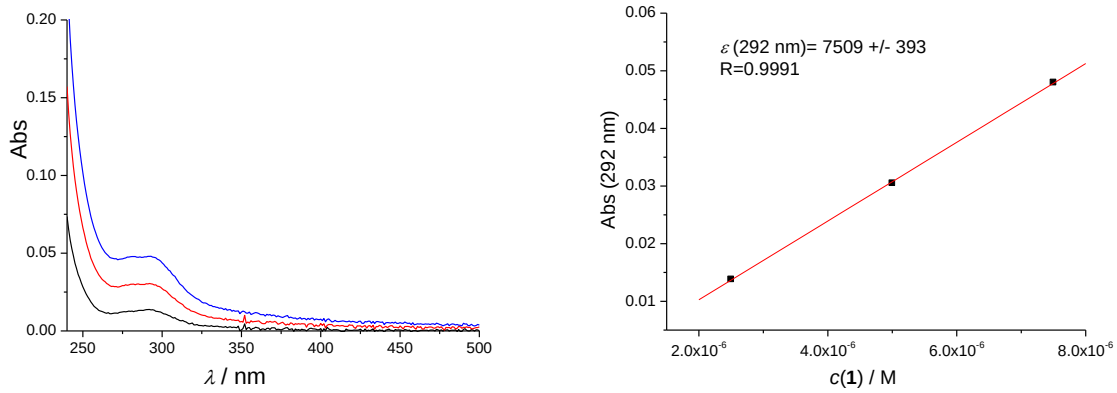

Figure S1. Concentration dependence of **1** UV/Vis spectrum in sodium cacodylate buffer pH 7, *I* = 0.05 M.

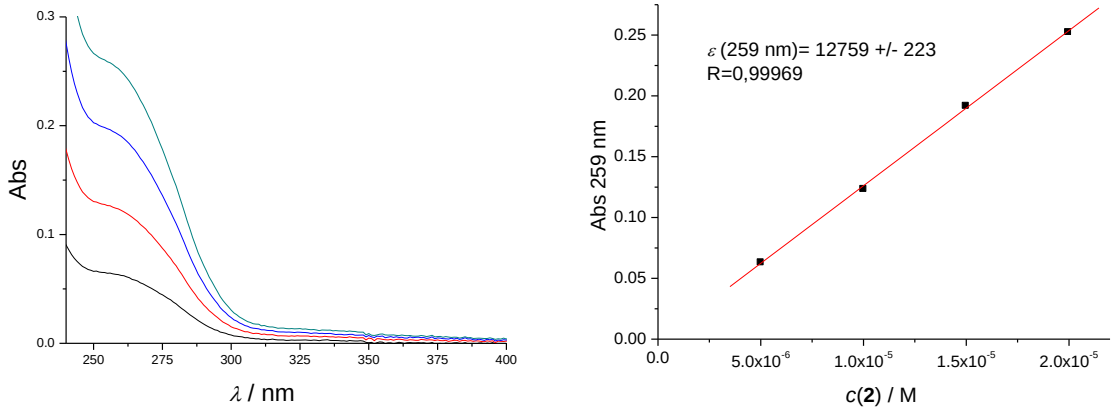

Figure S2. Concentration dependence of **2** UV/Vis spectrum in buffered solution pH 7, *I* = 0.05 M.

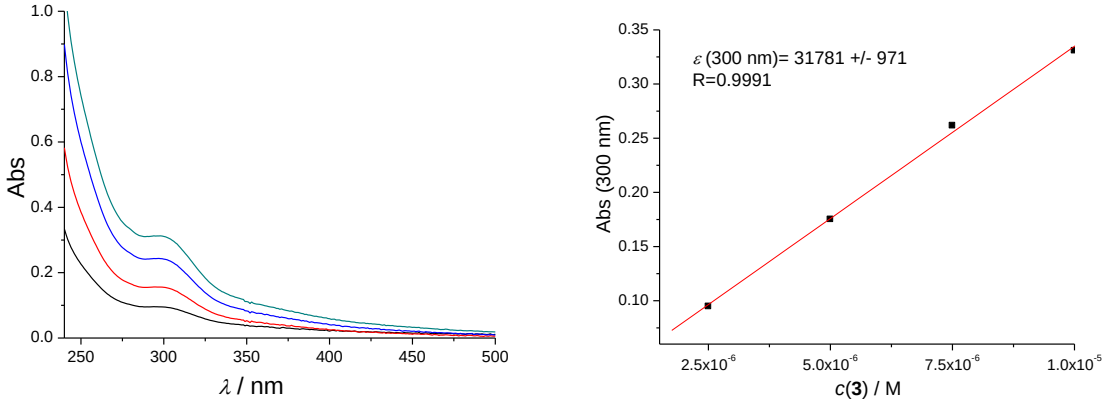

Figure S3. Concentration dependence of **3** UV/Vis spectrum in sodium cacodylate buffer pH 7, *I* = 0.05 M.

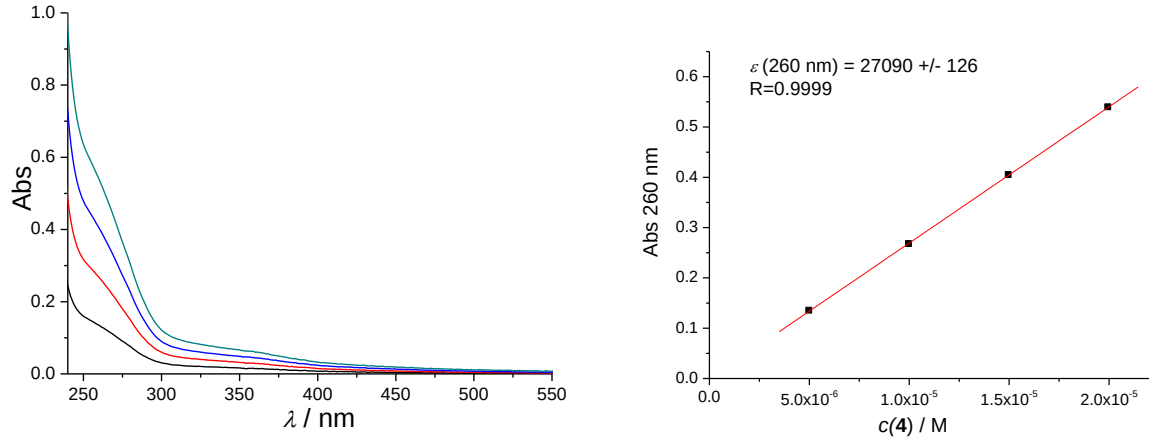

Figure S4. Concentration dependence of **4** UV/Vis spectrum in sodium cacodylate buffer pH 7, *I* = 0.05 M.

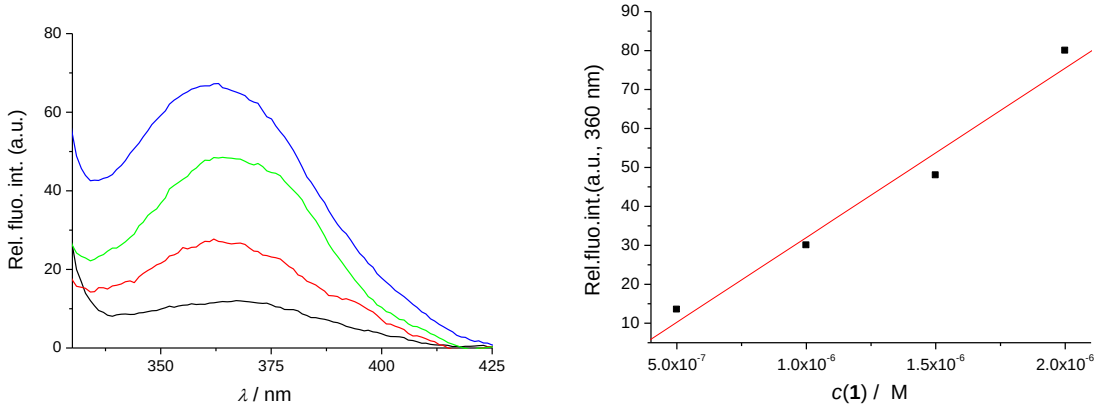

Figure S5. Fluorescence spectra of **1** (λ_{exc} = 300 nm) at micromolar concentrations, in buffer sodium cacodylate (pH 7.0, *I* = 0.05 M). Note baseline increase >420 nm for the highest concentration, attributed to colloidisation.

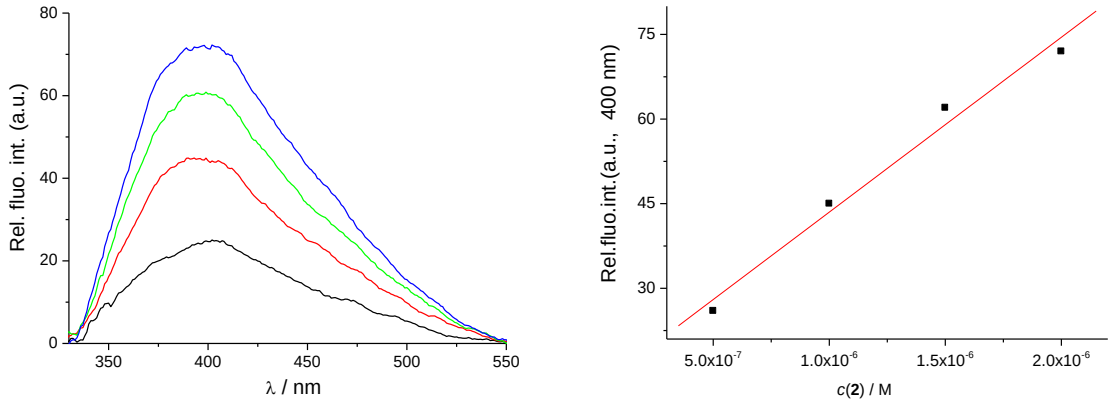

Figure S6. Fluorescence spectra of **2** (λ_{exc} = 300 nm) at micromolar concentrations, in buffer sodium cacodylate (pH 7.0, *I* = 0.05 M*).*

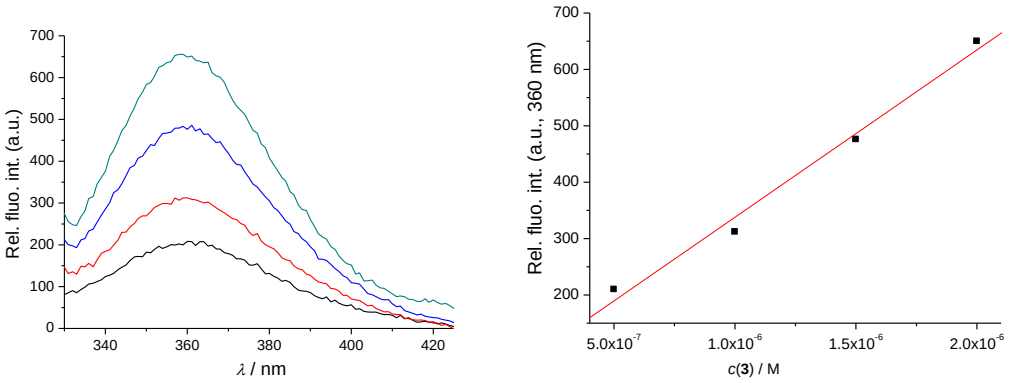

Figure S7. Fluorescence spectra of **3** (λ_{exc} = 300 nm) at micromolar concentrations, in buffer sodium cacodylate (pH 7.0, *I* = 0.05 M). Note baseline increase >420 nm for the highest concentration, attributed to colloidisation.

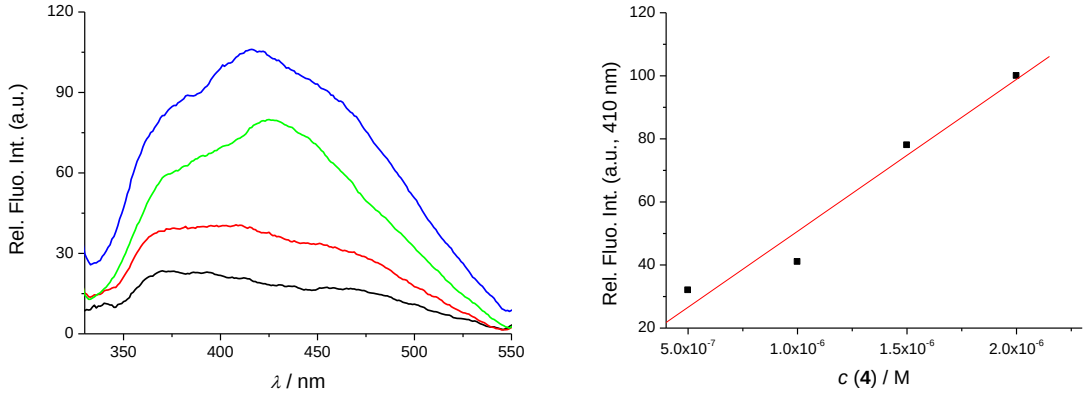

Figure S8. Fluorescence spectra of **4** (λ_{exc} = 300 nm) at micromolar concentrations, in buffer sodium cacodylate (pH 7.0, *I* = 0.05 M).

Relative quantum yields of fluorescence (Φ_f) were measured at room temperature (25 ºC) in sodium cacodylate buffer, pH 7, I = 0.05 M, by use of the fluorescence standard with optical properties closely matching the samples **1-4**: NATA (N-acetyl tryptophan amide) [3]. Before the measurements, the solutions were purged with Argon for 30 min. The concentrations were adjusted to absorbances of less than 0.1 at the excitation wavelengths of 270, 280 and 290 nm.

Fluorescence quantum yield was calculated according to:

$$\Phi_f = \Phi_{Ref}\left(\frac{n}{n_R}\right)^2 \frac{I}{I_R}\frac{1-10^{-A_R}}{1-10^{-A}} \qquad (S1)$$

Φ_f and Φ_{Ref} – fluorescence quantum yield of compound and the reference;
n and n_R – refractive index of the solvent in which compound or the reference was dissolved;
A and A_R – absorbance of the compound and the reference at the excitation wavelength;
I and I_R – area under emission curve of the compound and the reference

Table S2. Relative quantum yields (Φf) of calixarenes **1-4** determined in comparison to NATA (*N*-acetyl-L-tryptophanamide, Φ_R=0.14, λ_{exc} = 280 nm) standard[3].

λ_{exc} / nm	**1**	**2**	**3**	**4**
270	[b]0.0003	[b]0.0008	0.0029±0.001	[b]0.0003
280	[b]0.0003	0.0011±0.001	0.0031±0.001	[b]0.0002
290	[b]0.0005	0.0027±0.001	0.0047±0.001	[b]0.0008

[a] Fluorescence quantum yield estimated using NATA as a standard. The fluorescence spectra were measured by exciting at 270, 280 and 290 nm. The measurements were performed three times and the average values are reported. The associated errors correspond to the maximum absolute deviation; [b] Estimated values due to too low intensity of emission, generally could be considered as $\Phi f < 0.001$.

[3] M. G. Gore, Spectrophotometry and Spectrofluorimetry. A Practical Approach, Oxford University Press, 2000, p. 57.

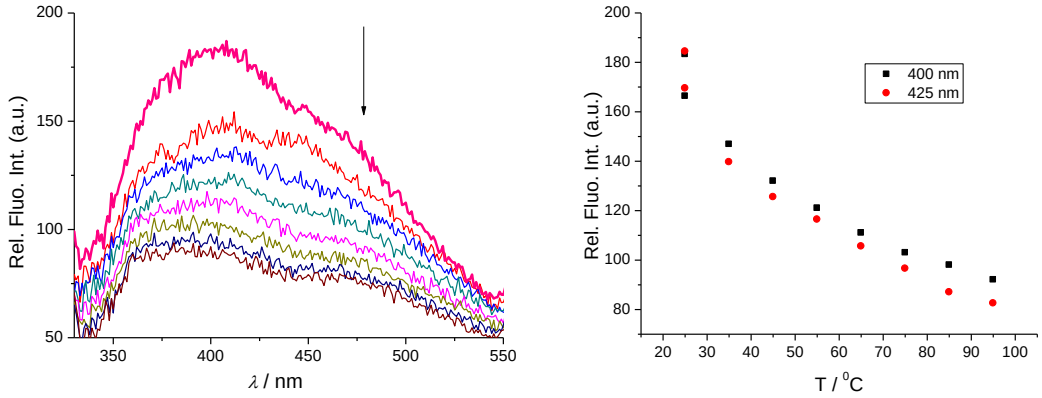

Figure S9. Temperature dependence (temperature range from 25 to 95°C) of emission of **4** (c = 2×10^{-6} M). Note excellent recovery upon cooling back to 25°C.

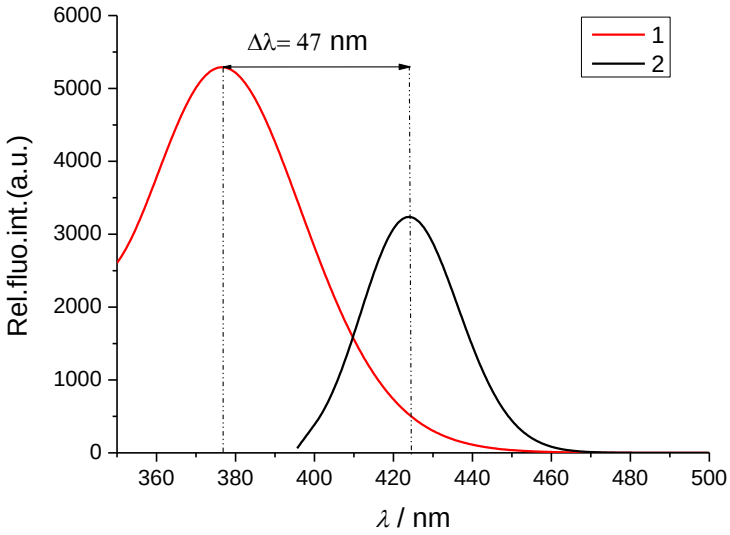

Figure S10. Comparison of calculated fluorescence spectra for compounds **1** and **2** obtained by TD-DFT (PCM/B3LYP/6-31G(d)). $\lambda_{em}(1)$ = 376 nm, $\lambda_{em}(2)$ = 423 nm.

3. Fluorimetric titrations with nucleotides:

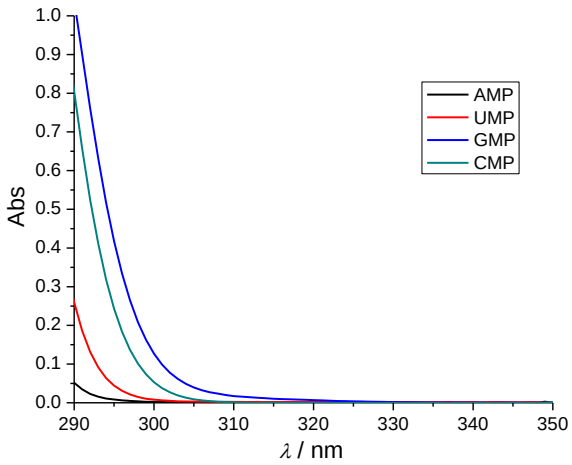

Figure S11. UV/vis spectra of mononucleotides (c = 10^{-3} M) at pH 7.0; sodium cacodylate buffer, I = 0.05 M.

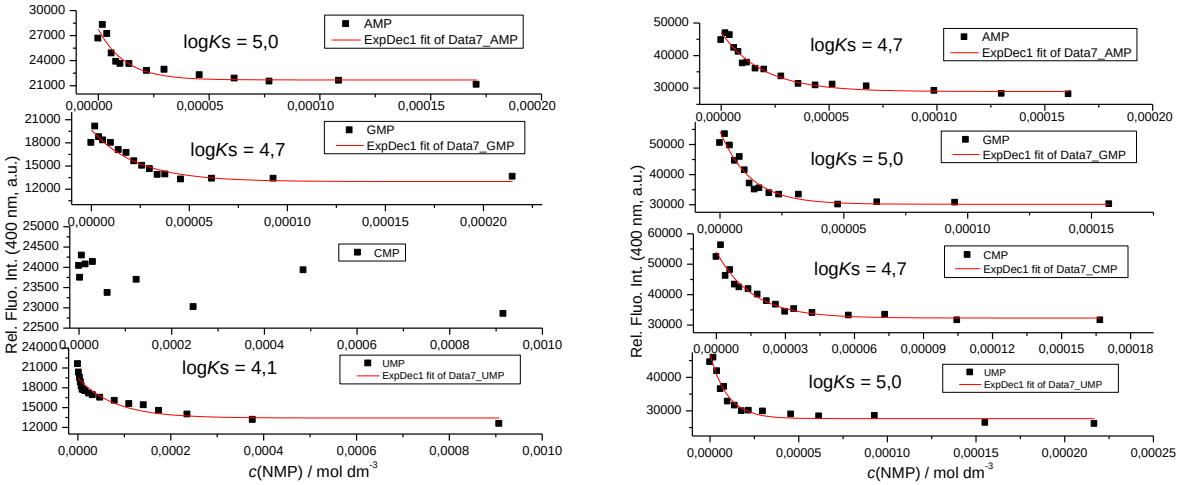

Figure S12**.** Changes in fluorescence of: **LEFT**) **1** (λ_{exc} = 300 nm, λ_{em} = 400 nm, c = 1 × 10^{-5} M) or **RIGHT**) **3** (λ_{exc} = 300 nm, λ_{em} = 400 nm, c = 1 × 10^{-6} M); upon addition of nucleotides. Done at pH 7.0; sodium cacodylate buffer, I = 0.05 M. Note that titrations were performed on Edinburgh FS5 instrument due to its superior sensitivity, and y-axis relative values differ from other figures, at which emission spectra were collected on Agilent Eclipse fluorimeter.

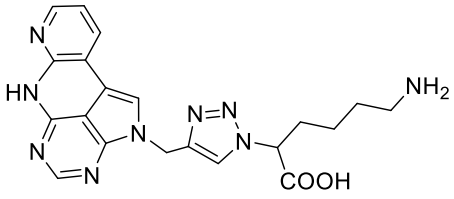

D8-111TFA–fluorescent nucleobase “clicked” to lysine

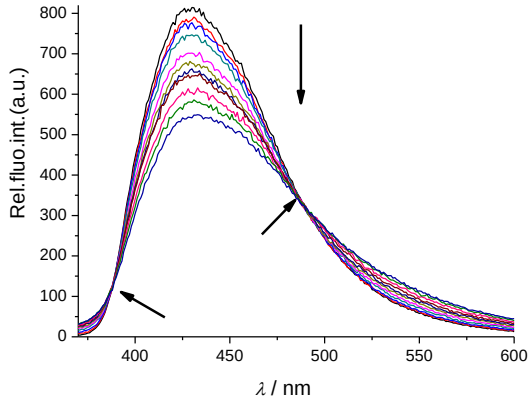

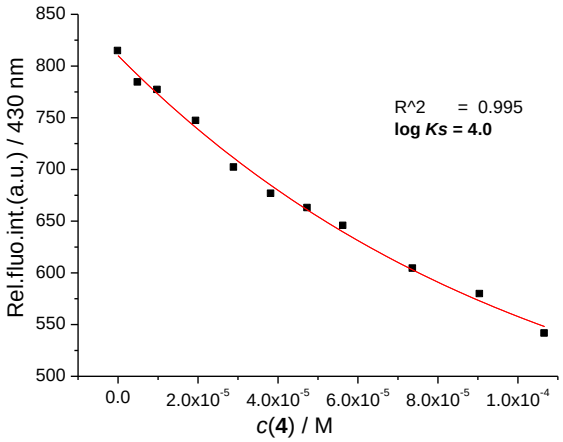

Figure S13 LEFT: Fluorimetric titration of **D8-111TFA** (c = 5×10^{-6} M; λ_{exc}= 350 nm) with **4** (c = 5×10^{-6} M) in buffer sodium cacodylate (pH 7.0, I = 0.05 M). RIGHT: Dependence of fluorescence at λ_{max} = 430 nm on c(BC135).

4. Titrations with DNA/RNA – displacement experiments

Description of the procedure: λ_{exc}= 520 nm; 2 mL quartz cuvette

Polynucleotide in cuvette $c = 5\times10^{-5}$ M, emission at 600 nm Int = 0

EB in cuvette, $c = 5\times10^{-6}$ M; emission at 600 nm collected

Polynucleotide/EB in cuvette (ratio EB/DNA = 0,1); emission spectrum collected,

Successive additions of studied compound, for ratio [EB] / [cpd.] = 1 – 0,1 emission at 600 nm collected

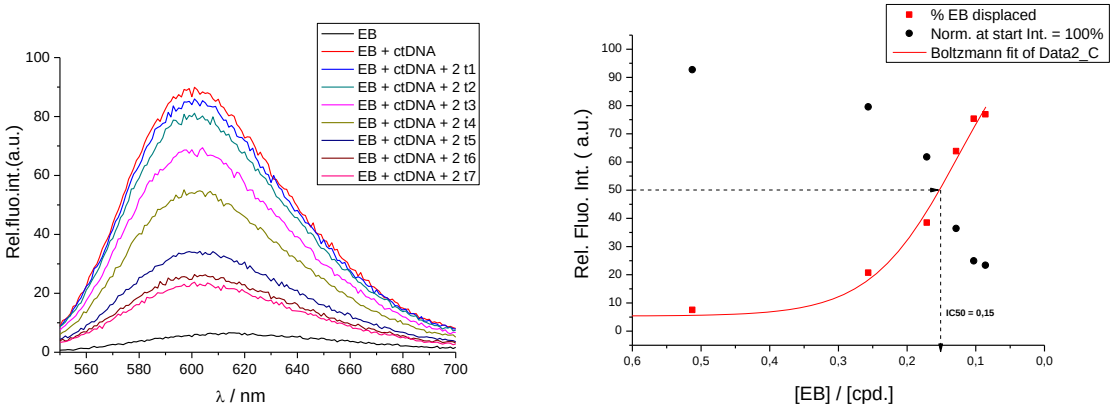

Figure S14. Ethidium bromide displacement ($c = 5\times10^{-6}$ M; λ_{exc}= 520 nm) from **ctDNA** ($c = 1\times10^{-6}$ M) with **2**, in buffer sodium cacodylate (pH 7.0, I = 0.05 M).

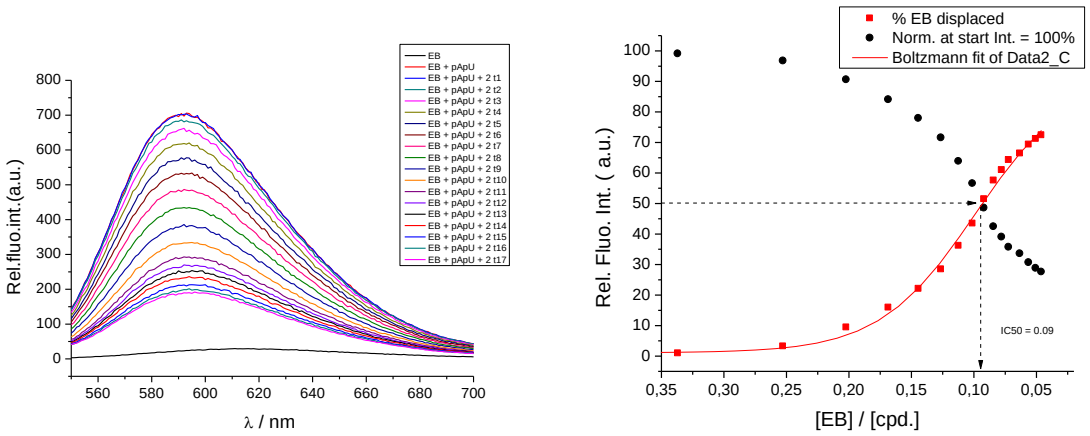

Figure S15. Ethidium bromide displacement ($c = 5\times10^{-6}$ M ; λ_{exc}= 520 nm) after binding with **poly A – poly U**, with **2** ($c = 5\times10^{-6}$ M), in buffer sodium cacodylate (pH 7.0, I = 0.05 M).

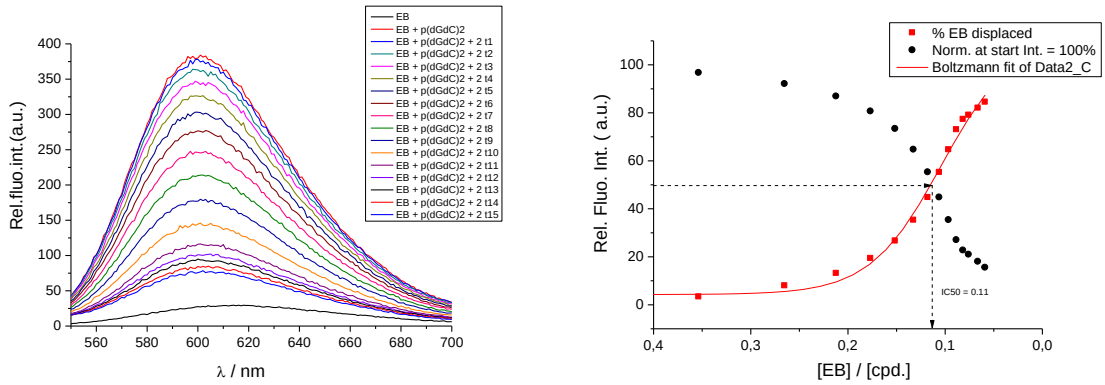

Figure S16. Ethidium bromide displacement (c = 5×10^{-6} M ; λ_{exc}= 520 nm) after binding with **poly dGdC – poly dGdC**, with **2** (c = 5×10^{-6} M), in buffer sodium cacodylate (pH 7.0, I = 0.05 M).

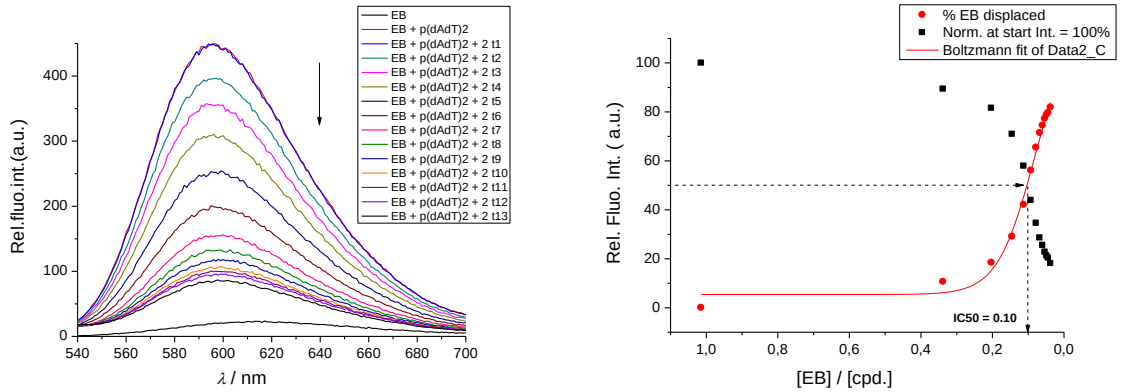

Figure S17. Ethidium bromide displacement (c = 5×10^{-6} M ; λ_{exc}= 520 nm) after binding with **poly dAdT – poly dAdT**, with **2** (c = 5×10^{-6} M), in buffer sodium cacodylate (pH 7.0, I = 0.05 M).

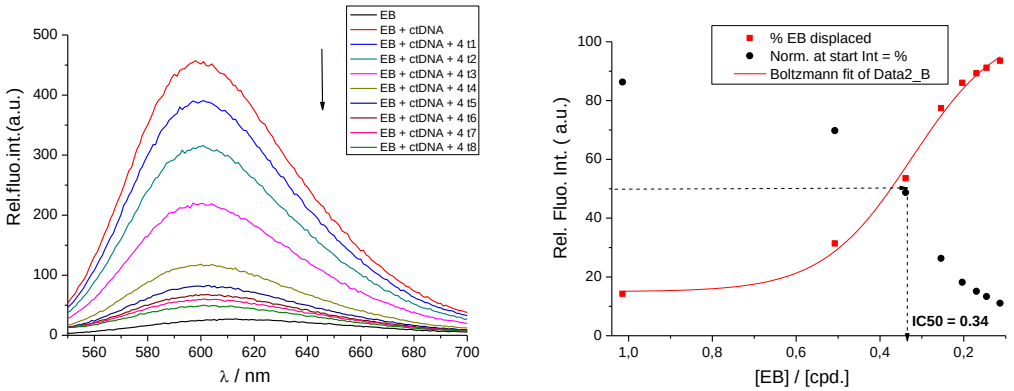

Figure S18. Ethidium bromide displacement (c = 5×10^{-6} M ; λ_{exc}= 520 nm) after binding with **ctDNA**, with **4** (c = 5×10^{-6} M), in buffer sodium cacodylate (pH 7.0, I = 0.05 M).

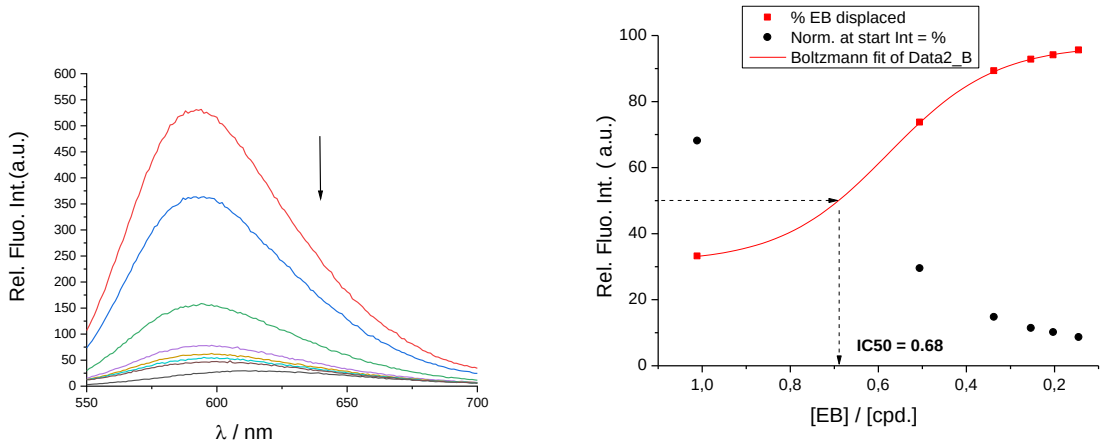

Figure S19. Ethidium bromide displacement (c = 5×10^{-6} M ; λ_{exc}= 520 nm) after binding with **poly A – poly U**, with **4** (c = 5×10^{-6} M), in buffer sodium cacodylate (pH 7.0, I = 0.05 M).

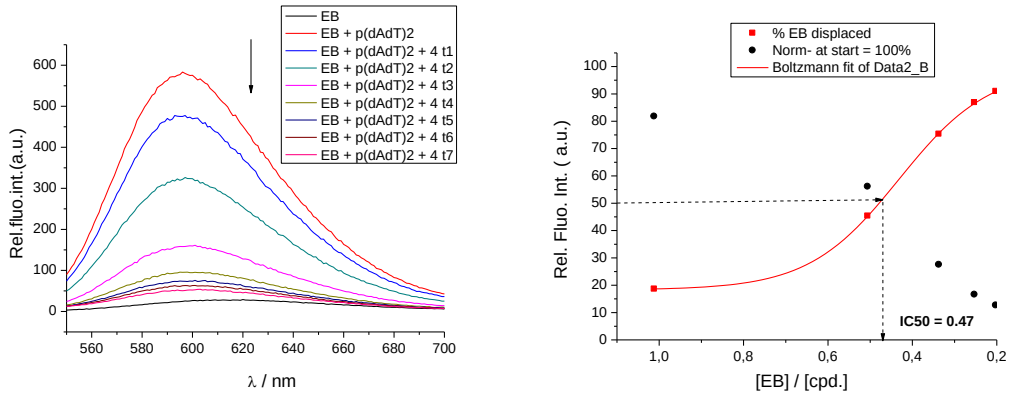

Figure S20. Ethidium bromide displacement (c = 5×10^{-6} M ; λ_{exc}= 520 nm) after binding with **poly dAdT – poly dAdT**, with **4** (c = 5×10^{-6} M), in buffer sodium cacodylate (pH 7.0, I = 0.05 M).

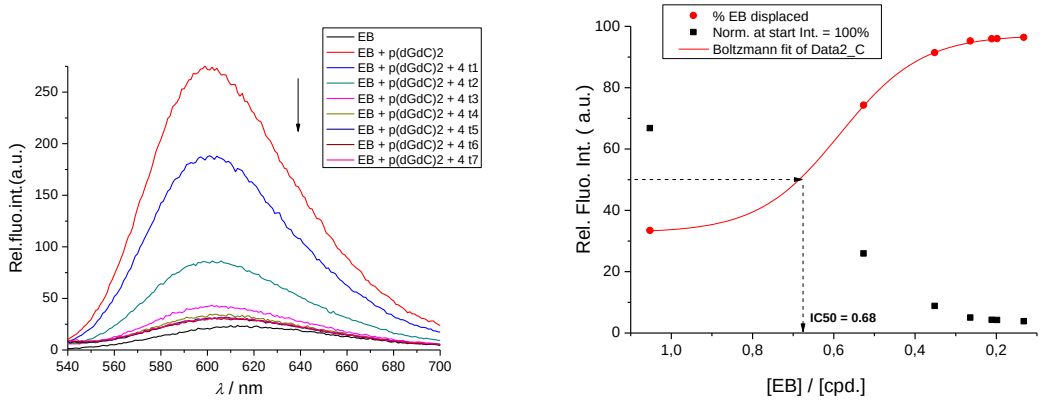

Figure S21. Ethidium bromide displacement (c = 5×10^{-6} M ; λ_{exc}= 520 nm) after binding with **poly dGdC – poly dGdC**, with **4** (c = 5×10^{-6} M), in buffer sodium cacodylate (pH 7.0, I = 0.05 M).

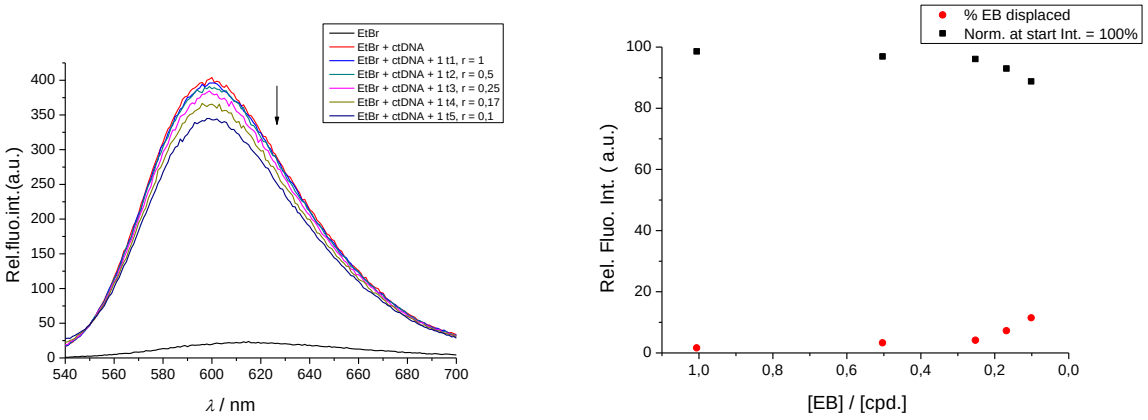

Figure S22. Ethidium bromide displacement (c = 5×10^{-6} M ; λ_{exc}= 520 nm) after binding with **ctDNA** (c = 5×10^{-5} M), with **1** (c = 5×10^{-6} M), in buffer sodium cacodylate (pH 7.0, I = 0.05 M). No measurable change in Rel. Fluo. Int.

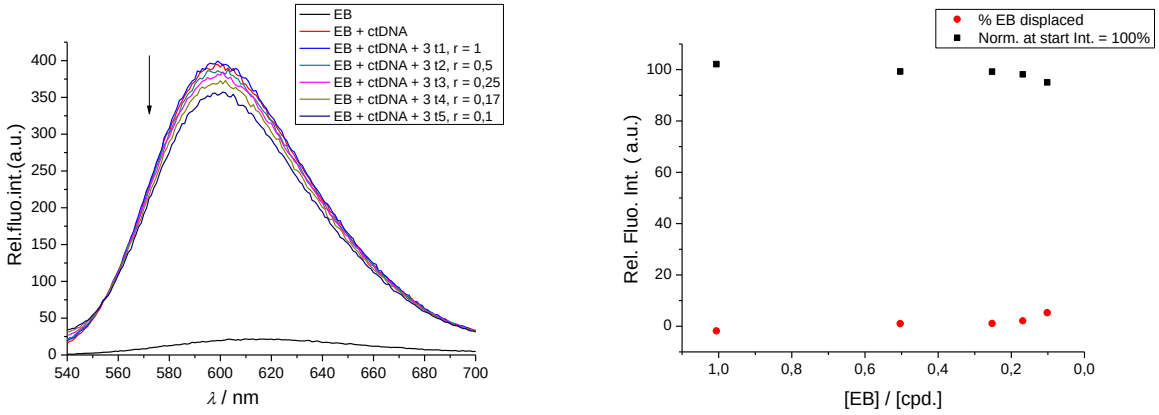

Figure S23. Ethidium bromide displacement (c = 5×10^{-6} M ; λ_{exc}= 520 nm) after binding with **ctDNA** (c = 5×10^{-5} M), with **3** (c = 5×10^{-6} M), in buffer sodium cacodylate (pH 7.0, I = 0.05 M).

5. Thermal denaturation experiments

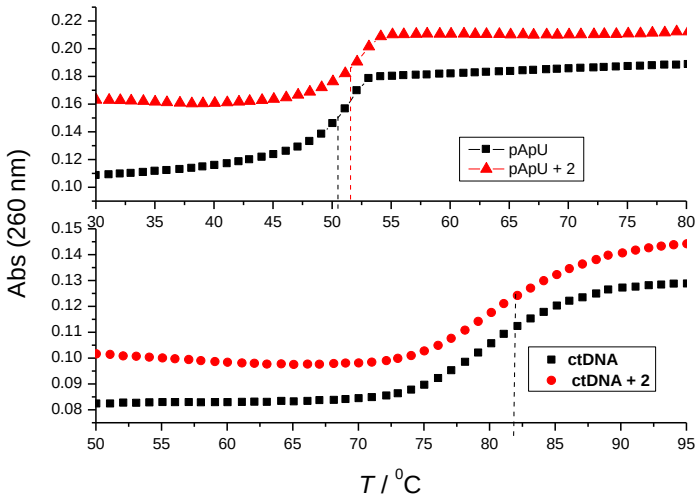

Figure S24. Thermal denaturation curves of **ct-DNA** (*c*(ct-DNA) = 2.5 × 10^{-5}M, $r_{[(2)]/[ct\text{-}DNA]}$ = 0.3) and **poly A - poly U** (*c*(pApU) = 2.5 × 10^{-5}M, $r_{[(2)]/[ct\text{-}DNA]}$ = 0.3) at pH 7.0 (sodium cacodylate buffer, *I* = 0.05 M) upon addition of **2**. Error in ΔTm values: ±0.5 °C.

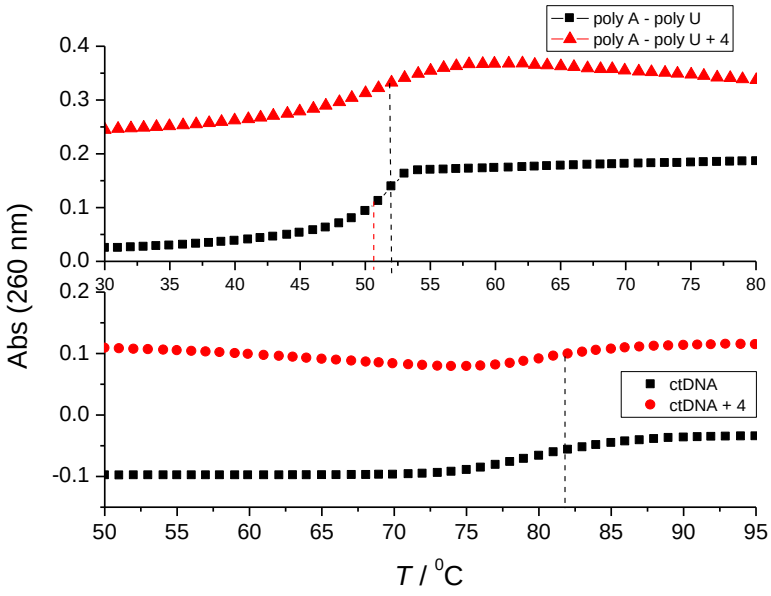

Figure S25. Thermal denaturation curves of **ct-DNA** (*c*(ct-DNA) = 2.5 × 10^{-5}M, $r_{[(4)]/[ct\text{-}DNA]}$ = 0.3) and **poly A - poly U** (*c*(pApU) = 2.5 × 10^{-5}M, $r_{[(4)]/[ct\text{-}DNA]}$ = 0.3) at pH 7.0 (sodium cacodylate buffer, *I* = 0.05 M) upon addition of **4**. Error in ΔT_m values: ±0.5 °C.

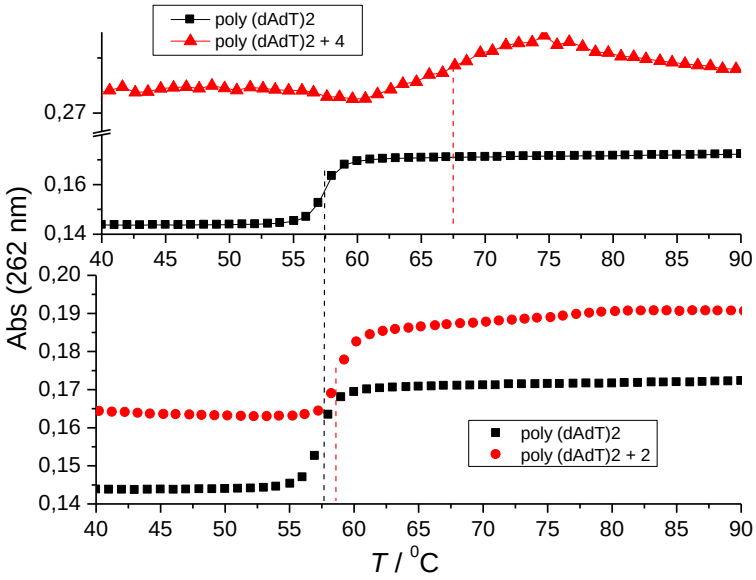

Figure S26. Thermal denaturation curves of **poly (dAdT)$_2$** (c(p(dAdT)$_2$) = 2.5 × 10^{-5} M, $r_{[(\text{cpd.})]/[\text{p(dAdT)2}]}$ = 0.3) at pH 7.0 (sodium cacodylate buffer, I = 0.05 M) upon addition of **2** and **4**. Error in ΔT_m values: ±0.5 °C.

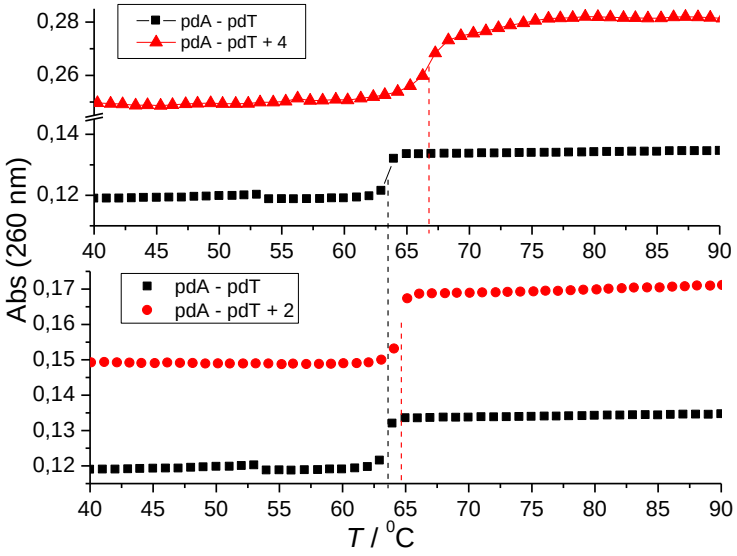

Figure S27. Thermal denaturation curves of **poly dA – poly dT** (c(p(dAdT)) = 2.5 × 10^{-5} M, $r_{[(\text{cpd.})]/[\text{p(dAdT)2}]}$ = 0.3) at pH 7.0 (sodium cacodylate buffer, I = 0.05 M) upon addition of **2** and **4**. Error in ΔT_m values: ±0.5 °C.

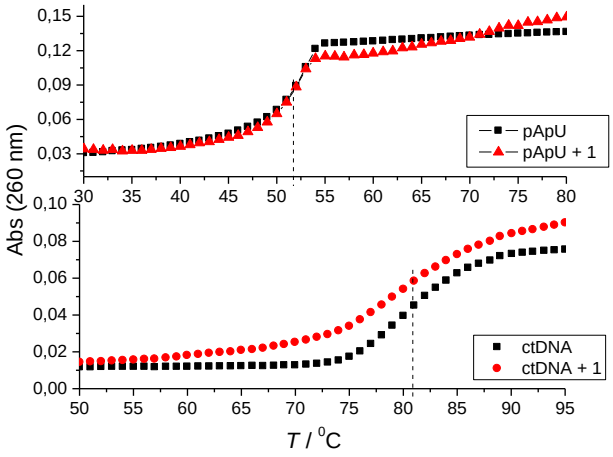

Figure S28. Thermal denaturation curves of **ctDNA** (c(ctDNA) = 2.5 × 10^{-5}M, $r_{[(1)]/[ctDNA]}$ = 0.3) and **poly A - poly U** (c(pApU) = 2,5 × 10^{-5}M, $r_{[(1)]/[pApU]}$ = 0.3) at pH 7.0 (sodium cacodylate buffer, I = 0.05 M) upon addition of **1**. Error in ΔTm values: ±0.5 °C.

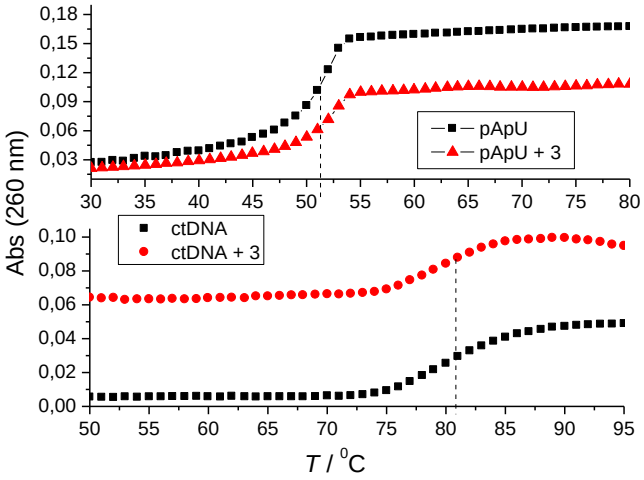

Figure S29. Thermal denaturation curves of **ctDNA** (c(ctDNA) = 2.5 × 10^{-5}M, $r_{[(3)]/[ctDNA]}$ = 0.3) and **poly A - poly U** (c(pApU) = 2.5 × 10^{-5} M, $r_{[(3)]/[pApU]}$ = 0.3) at pH 7.0 (sodium cacodylate buffer, I = 0.05 M) upon addition of **3**. Error in ΔTm values: ±0.5 °C

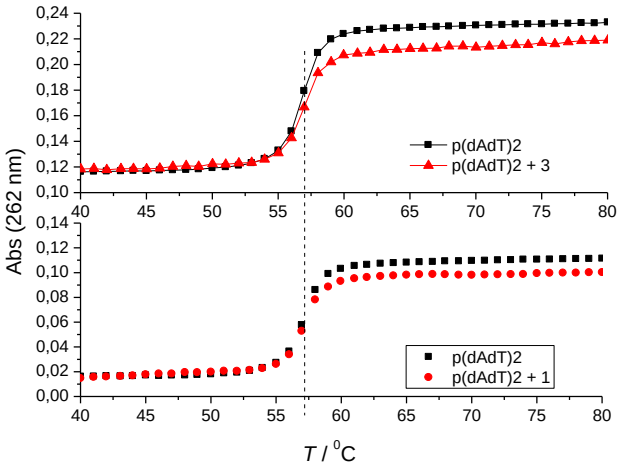

Figure S30. Thermal denaturation curves of **p(dAdT)$_2$** (c(p(dAdT)$_2$) = 2,5 × 10^{-5} M, $r_{[(\mathbf{cmp})]/[\mathbf{p(dAdT)2}]}$ = 0.3) (sodium cacodylate buffer, I = 0.05 M) upon addition of **1** and **3**. Error in ΔTm values: ±0.5 °C

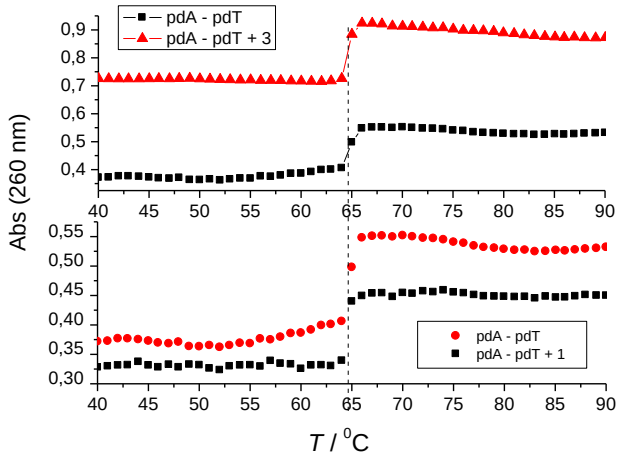

Figure S31. Thermal denaturation curves of **pdA – pdT** (c(pdA - pdT) = 2,5 × 10^{-5} M, $r_{[(\mathbf{cmp})]/[\mathbf{pdA\text{-}pdT}]}$ = 0.3) (sodium cacodylate buffer, I = 0.05 M) upon addition of **1** and **3**. Error in ΔTm values: ±0.5 °C

6. Circular dichroism (CD) experiments

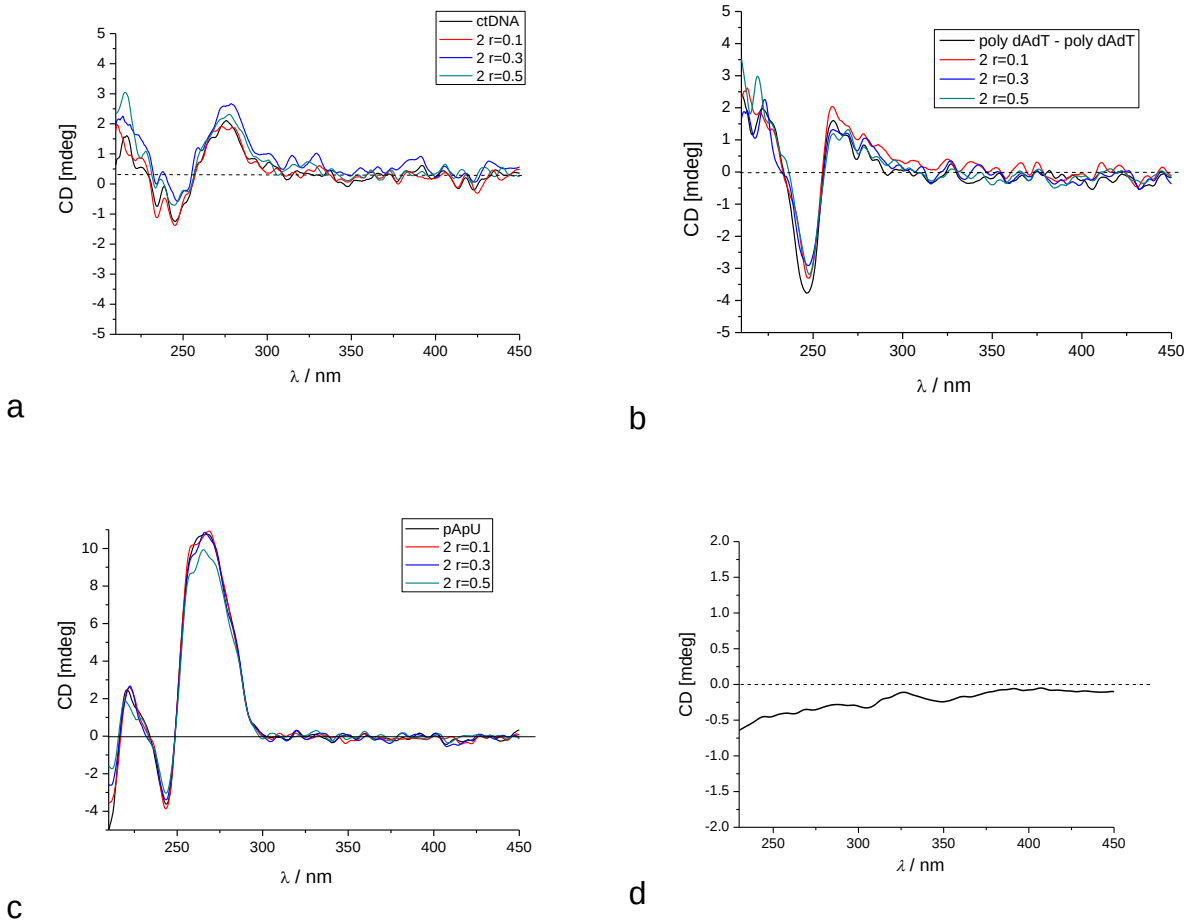

Figure S32. **a-c)** CD titration of ct-DNA, poly $(dAdT)_2$ and poly A – poly U (all DNA/RNA *c* = 2×10^{-5} M) with **2** at molar ratios ***r*** = 0,1; 0,3 and 0,5 (*r* = [compound] / [polynucleotide]). **d)** CD spectra of **2** (*c* = 1×10^{-5} M). All CD experiments were done in sodium cacodylate buffer (pH 7.0, *I* = 0.05 M).

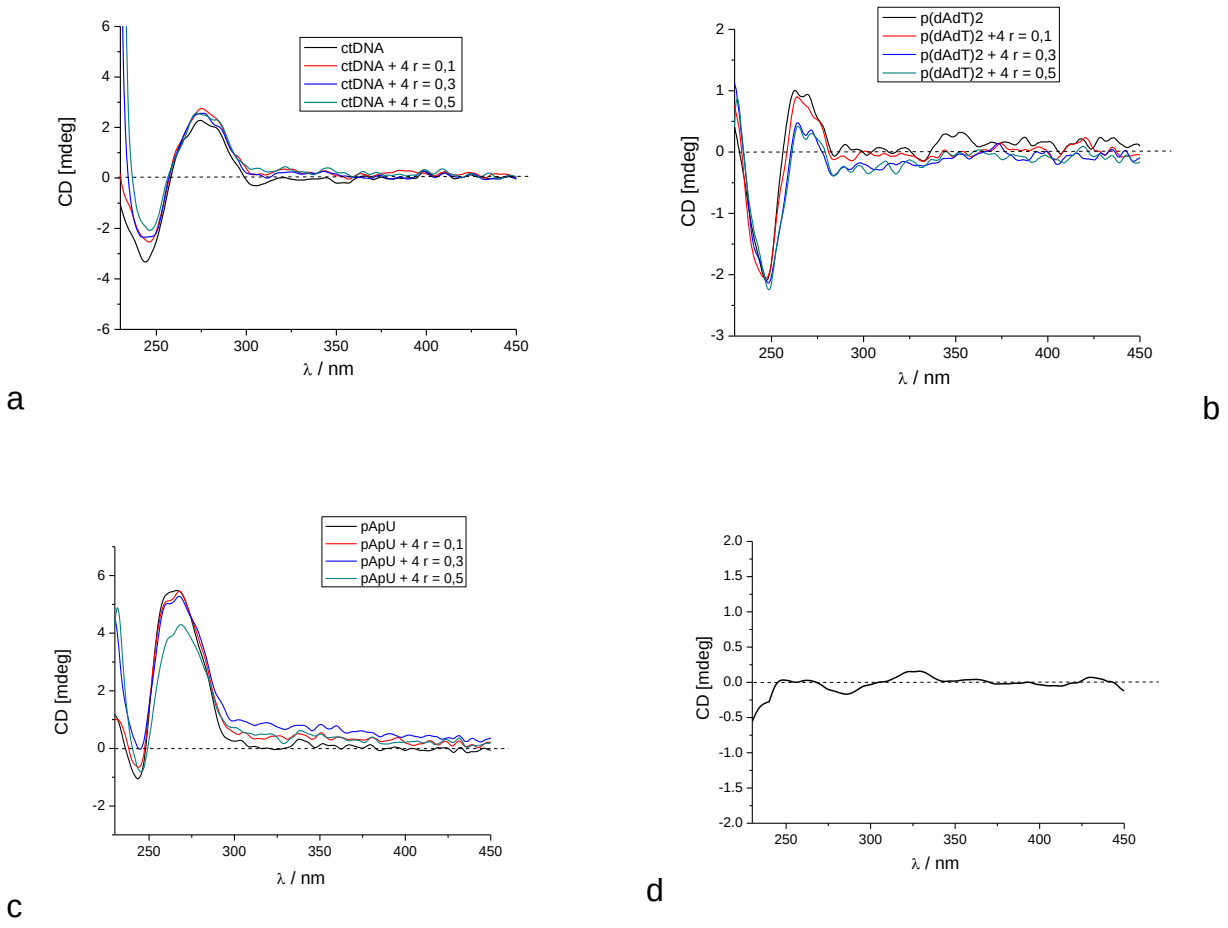

Figure S33. **a-c)** CD titration of ctDNA, poly $(dAdT)_2$ and poly A – poly U (all DNA/RNA *c* = 2×10^{-5} M) with **4** at molar ratios ***r*** = 0,1; 0,3 and 0,5 (*r* = [compound] / [polynucleotide]). **d)** CD spectra of **4** (*c* = 1×10^{-5} M). All CD experiments were done in sodium cacodylate buffer (pH 7.0, *I* = 0.05 M).

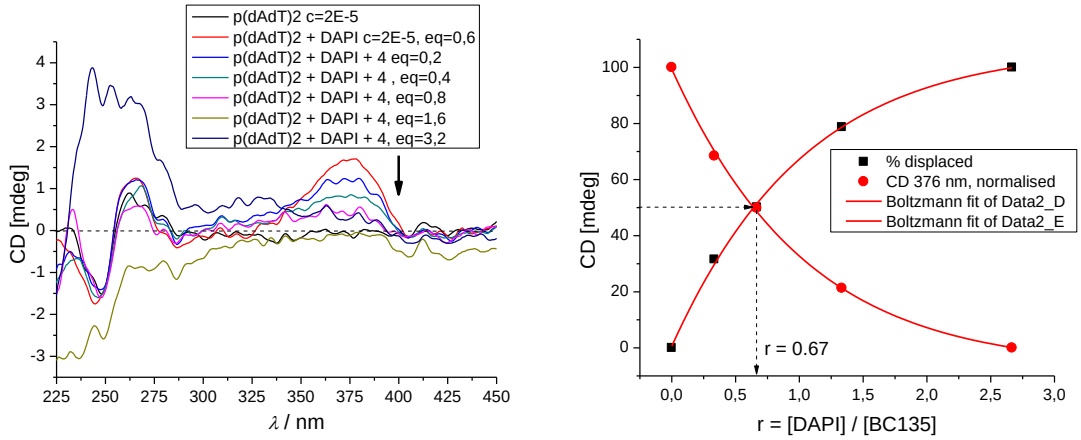

Figure S34. DAPI displacement (c = 2×10^{-5} M) with **4** (c = 2×10^{-5} M) after binding to poly (dAdT)$_2$ in buffer sodium cacodylate (pH 7.0, I = 0.05 M).

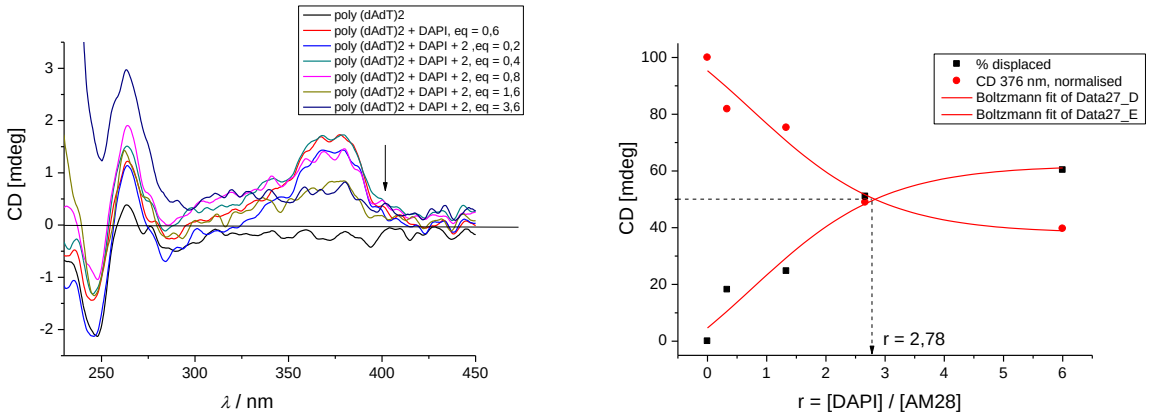

Figure S35. DAPI displacement (c = 2×10^{-5} M) with **2** (c = 2×10^{-5} M) after binding to poly (dAdT)$_2$ in buffer sodium cacodylate (pH 7.0, I = 0.05 M).